Electronic Supplementary Material (ESI) for ChemComm.
This journal is © The Royal Society of Chemistry 2023

Electronic Supplementary Information

Excitonic coupling of RNA-templated merocyanine dimer studied by higher-order transient absorption spectroscopy

Julia Dietzsch,[a#] Ajay Jayachandran,[b#] Stefan Mueller,[b] Claudia Höbartner[a,c*] and Tobias Brixner[b,c*]

[a]Institut für Organische Chemie, Universität Würzburg, Am Hubland, 97074 Würzburg, Germany

[b]Institut für Physikalische und Theoretische Chemie, Universität Würzburg, Am Hubland, 97074 Würzburg, Germany

[c]Center for Nanosystems Chemistry (CNC), Universität Würzburg, Theodor-Boveri-Weg, 97074 Würzburg, Germany

[#]These authors contributed equally.

*Corresponding authors:

Claudia Höbartner, claudia.hoebartner@uni-wuerzburg.de

Tobias Brixner, brixner@uni-wuerzburg.de

1. Materials and methods

All standard chemicals and solvents were purchased from commercial suppliers. Organic solvents were used in *pro analysis* or for synthesis quality without further purification while solvents for column chromatography were purchased in technical quality and distilled prior to use. Dry solvents (dichloromethane, DMF, acetonitrile) were obtained from a solvent purification system (SPS). Nanopure water was obtained from a Sartorius Arium® pro ultrapure water system. Thin layer chromatography (TLC) was performed on silica gel pre-coated aluminum plates (Alugram SIL G/UV254, Macherey-Nagel). Visualization was accomplished by irradiation with UV light at 254 nm. 4,4'-Dimethoxytrityl(DMT)-protected compounds were stained with 5% sulfuric acid in ethanol. Column chromatography was carried out on silica gel (Kieselgel 60, Merck, 0.063 – 0.200 mm). Standard 5'-*O*-DMT-2'-*O*-TOM-protected RNA phosphoramidites for solid phase synthesis as well as standard 5'-*O*-DMT-protected CPG supports (1000 Å, 25-35 µmol/g) were purchased from ChemGenes or Sigma Aldrich.

NMR spectra were measured on a Bruker Avance III HD 400 spectrometer at 400 MHz. Chemical shifts (δ) were referenced to the residual solvent signals as internal standards (in ppm; $CDCl_3$: ^1H = 7.26, ^{13}C = 77.16, DMSO: ^1H = 2.50, ^{13}C = 39.52) or on the unified scale for ^{31}P. Coupling constants (J) were reported in Hz. Multiplets were abbreviated as follows: s (singlet), d (doublet), t (triplet), q (quartet) and m (multiplet). Spectral assignments were verified by 2D NMR experiments. High resolution ESI mass spectra were measured on a Bruker micrOTOF-Q III spectrometer and monoisotopic masses for oligonucleotides were obtained by charge deconvolution of the raw spectra.

2. Synthesis of the rBAM2 phosphoramidite building block

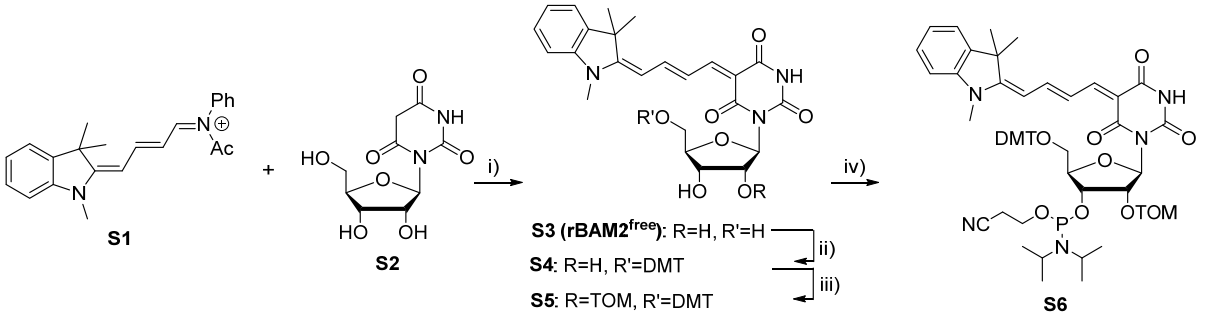

Scheme S1. Reagents and conditions for the synthesis of the rBAM phosphoramidite building block **S6**. Compound **S1** and **S2** were prepared according to reported procedures[1-3]. i) NEt_3, EtOH, r. t., 30 min (76%); ii) 1. DMF-DMA, pyridine, r. t., 20 h 2. DMT-Cl, pyridine, r. t., 3 h (75%); iii) 1. DIPEA, $^nBu_2SnCl_2$, DCE, 80 °C, 40 min. 2. TOM-Cl, r. t., 1.5 h (25%); iv) 2-cyanoethyl-*N,N*-diisopropylchlorophosphoramidite, *N*-ethyl-*N,N*-dimethylamine, DCM, r. t., 3 h (32%).

The synthesis of the rBAM2 phosphoramidite building block for RNA solid-phase synthesis shown in Scheme S1 started with and aldol-type reaction of the activated chromophore precursor **S1** (prepared from 1,2,3,3-tetramethylindolinium iodide and *N*-[3-(phenylamino)-2-propen-1-ylidene]benzenamine[1, 2]) and the free barbituric acid nucleoside **S2**[3] to the free rBAM2 nucleoside (**S3, rBAM**^{free}). Subsequent in situ 2',3'-acetal protection followed by 5'-tritylation under standard reaction conditions provided compound **S4**. 2'-Silyl protection gave derivative **S5** along with the 3'-TOM-protected isomer. Compound **S5** was then converted into the target phosphoramidite **S6** by 3'-phosphitylation. Purification by column chromatography resulted in lower yields than for standard nucleosides, likely due to the sensitivity of rBAM2 towards nucleophiles. The yields have not been further optimized, and the final product was used for solid-phase synthesis.

2.1 Barbituric acid merocyanine ribonucleoside S3 (rBAM2^{free})

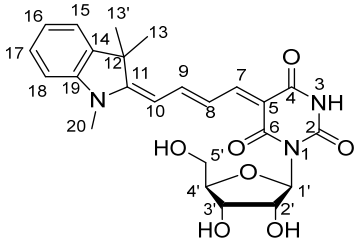

The barbituric acid nucleoside **S2** (1.05 g, 4.04 mmol, 1.00 eq.) and compound **S1** (1.86 g, 4.85 mmol, 1.20 eq.) were dissolved in absolute ethanol (75 mL). Triethylamine (1.60 mL, 11.4 mmol. 2.82 eq.) was added and the reaction mixture was stirred for 30 min at r. t., resulting in the formation of a deeply pink solution. The solvent was removed in vacuum and the residue was purified by column chromatography on silica gel (DCM/MeOH 9:1) to yield the final product **S3** as a dark solid (1.37 g, 3.06 mmol, 76%).

Compound **S2** was obtained as a 1:1 mixture of (*E)* and (*Z*) double bond isomers which explains the two sets of signals in the ^{1}H NMR spectra of this and the following compounds.

^{1}H NMR (400 MHz, DMSO-d_6): δ (ppm) = 10.79 (2 s, 1 H, NH), 8.26 – 8.05 (m, 2 H, 7-H, 9-H), 7.74 – 7.57 (m, 1 H, 8-H), 7.56 – 7.47 (m, 1 H, arom. H), 7.41 – 7.26 (m, 2 H, arom. H), 7.17 (tt, *J* = 7.4, 1.4 Hz, 1 H, arom. H), 6.21 (t, *J* = 13.7 Hz, 1 H, 10-H), 6.06 (d, *J* = 3.5 Hz, 1 H, H-1'), 5.02 (d, *J* = 5.0 Hz, 1 H, 2'-OH), 4.82 (s, 1 H, 3'-OH), 4.61 (s, 1 H, 5'-OH), 4.45 (d, *J* = 5.7 Hz, 1 H, H-2'), 4.11 (s, 1, H-3'), 3.72 – 3.55 (m, 2 H, H-4', H-5'), 3.54 (d, *J* = 4.4 Hz, 3 H, NCH_3), 3.42 (d, *J* = 4.5 Hz, 1 H, H-5'), 1.62 (s, 6 H, 2×CH_3);

^{13}C{^{1}H} NMR (100 MHz, DMSO-d_6): δ (ppm) = 172.61 (C-11), 172.45 (C-11), 163.53 (carbonyl-C), 162.87 (carbonyl-C), 162.50 (carbonyl-C), 162.32 (carbonyl-C), 157.78 (C-9), 157.46 (C-9), 155.66 (C-7), 155.01 (C-7), 142.95 (arom. C), 140.72 (arom. C), 132.91 (arom. C), 129.28 (arom. C), 128.60 (arom. C), 128.22 (arom. C), 124.00 (arom. C), 122.21 (C-8), 121.00 (C-8), 120.47, 110.45, 110.39, 101.70 (10-C), 101.60 (10-c), 87.90 (1'-C), 87.79 (1'-C), 84.21 (4'-C), 84.02 (4'-C), 71.38 (2'-C), 70.21 (3'-C), 70.12 (3'-C), 62.52 (5'-C), 48.41, 48.37, 30.74 (C-20), 29.62, 27.16 (C-13, C13');

HR-MS (ESI^{+}): exact mass calculated for $C_{24}H_{27}N_3NaO_7$, [M+Na]$^{+}$): 492.17412, found: 492.17361.

2.2 5'-*O*-(4,4'-Dimethoxytrityl) barbituric acid merocyanine ribonucleoside S4

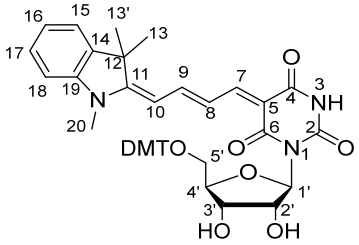

The barbituric acid merocyanine ribonucleoside **S3** (800 mg, 1.70 mmol, 1.00 eq.) was dissolved in dry pyridine (45 mL) under N_2-atmosphere and DMF-DMA (504 mg, 4.26 mmol, 2.50 eq.) was added. The mixture was stirred at r. t. for 20 h. Afterwards, the solvent was removed in vacuum and the residue re-dissolved in dry pyridine (45 mL) under N_2-atmosphere. DMT-Cl (691 mg, 2.04 mmol, 1.20 eq.) was added and the mixture was stirred at r. t. for 3 h. After addition of MeOH (5 mL) the reaction mixture was stirred for additional 20 min. The solvent was removed under reduced pressure and the crude product was purified via column chromatography on silica gel (DCM/MeOH 9:1) to obtain **S4** as a dark purple foam (978 mg, 1.27 mmol, 75%).

^{1}H NMR (400 MHz, DMSO-d_6) δ (ppm) = 10.80 (d, J = 28.4 Hz, 2 H), 8.59 (dt, J = 4.4, 1.7 Hz, 1 H), 8.23 – 8.05 (m, 3 H), 7.82 (tt, J = 7.7, 1.8 Hz, 1 H), 7.74 – 7.59 (m, 1 H), 7.55– 7.49 (m, 1 H), 7.44 – 7.33 (m, 5 H), 7.33 – 7.22 (m, 9 H), 7.22 – 7.15 (m, 3 H), 7.09 – 7.04 (m, 1 H), 6.89 – 6.80 (m, 5 H), 6.27 – 6.15 (m, 1 H), 6.11 (s, 2 H), 5.08 (s, 1 H), 4.82 (s, 1 H), 4.38 – 4.30 (m, 1 H), 4.28 – 4.11 (m, 1 H), 3.87 – 3.79 (m, 1 H), 3.74 – 3.68 (m, 8 H), 3.53 (s 3 H), 3.17 – 3.00 (m, 3 H), 1.62 (s, 8 H);

^{13}C{^{1}H} NMR (100 MHz, DMSO-d_6) δ (ppm) = 162.42, 158.04, 158.00, 157.87, 149.31, 145.17, 145.10, 143.00, 140.74, 140.29, 136.75, 135.90, 135.82, 135.76, 129.86, 129.77, 128.98, 128.28, 127.81, 127.70, 127.50, 126.61, 124.17, 122.25, 120.56, 113.16, 113.12, 112.83, 110.41, 101.58, 85.32, 79.97, 72.18, 70.33, 55.07, 55.04, 55.02, 48.45, 48.39, 27.21;

HR-MS (ESI^{+}): Exact mass calculated for $C_{45}H_{45}N_3O_9$ [M+H]$^{+}$: 771.31503, found: 771.31463.

2.3 5'-*O*-(4,4'-Dimethoxytrityl)-2'-*O*-tri-*iso*-propylsilyloxymethyl barbituric acid merocyanine ribonucleoside S5

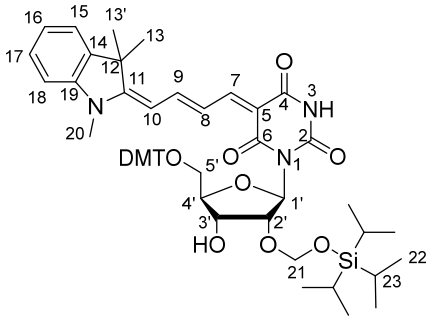

Merocyanine ribonucleoside **S4** (380 mg, 494 µmol, 1.00 eq.) and DIPEA (255 mg, 1.98 mmol, 4.00 eq.) were dissolved in dry DCE (4 mL) under N_2-atmosphere. $^nBu_2SnCl_2$ (448 mg, 1.48 mmol, 3.00 eq.) was added and the mixture was heated to 80 °C and stirred for 1 h at this temperature. TOM-Cl (132 mg, 593 µmol, 1.20 eq.) was added and the reaction mixure was stirred for additional 40 min. The solvent was removed under reduced pressure and the crude product was purified by column chromatography on silica gel (DCM/MeOH 97:3 to 95:5). The pure product **57** was obtained as a dark purple foam (119 mg, 124 µmol, 25%), along with an equal amount of the undesired 3'-silylated compound which both were identified by ^{1}H-^{1}H COSY NMR.

^{1}H NMR (400 MHz, $CDCl_3$) δ (ppm) = 8.11 – 7.99 (m, 1 H, 7-H), 7.93 – 7.69 (m, 3 H, 8-H, 9-H), 7.56 – 7.46 (m, 2 H), 7.42 – 7.32 (m, 5 H, DMT.H), 7.30 (d, *J* = 7.6 Hz, 1 H), 7.23 (tt, *J* = 6.4, 2.1 Hz, 2 H), 7.20 – 7.10 (m, 2 H), 6.97 (t, *J* = 6.5 Hz, 1 H), 6.83 – 6.74 (m, 4 H, DMT-H), 6.40 (t, *J* = 3.1 Hz, 1 H, H-1'), 5.95 (t, *J* = 13.3 Hz, 1 H, 10-H), 5.09 (dd, *J* = 4.8, 1.2 Hz, 1 H, 21-H), 4.97 (dd, *J* = 4.8, 2.2 Hz, 1 H, 21-H), 4.79 (ddd, *J* = 15.6, 6.6, 3.0 Hz, 1 H, H-2'), 4.59 – 4.43 (m, 1 H, H-3'), 3.96 (ddq, *J* = 10.4, 6.6, 3.4 Hz, 1 H, H-4'), 3.75 (dd, *J* = 3.3, 1.7 Hz, 7 H, 3'-OH, DMT-OCH_3), 3.47 – 3.31 (m, 5 H, H-5', 20-H), 2.99 – 2.94 (m, 2 H), 1.63 (d, *J* = 12.7 Hz, 11 H, 13-H), 1.25 (d, *J* = 1.4 Hz, 8 H, 22-H), 1.17 – 0.97 (m, 22 H, 23-H);

^{13}C{^{1}H} NMR (100 MHz, $CDCl_3$) δ (ppm) = 171.57 (11-C), 163.92 (2-C, 4-C, 6-C), 163.29 (2-C, 4-C, 6-C), 162.61 (2-C, 4-C, 6-C), 162.20 (2-C, 4-C, 6-C), 158.52, 158.50, 157.62 (7-C, 8-C), 157.41 (7-C, 8-C), 157.06 (7-C, 8-C), 156.97 (7-C, 8-C), 145.41, 143.17, 140.52, 136.72, 136.70, 136.66, 136.58, 130.51, 130.49, 130.47, 128.70, 128.66, 128.62, 127.91, 126.74, 124.32 (DMT-C), 122.33 (9-C), 122.17 (9-C), 121.84 (9-C), 113.22 (DMT-C), 109.45, 101.09 (10-C), 90.52 (21-C), 90.47 (21-C), 86.28 (1'-C), 86.23 (1'-C), 83.38 (4'-C), 83.19 (4'-C), 79.77 (2'-C), 70.75 (3'-C), 70.49 (3'-C), 64.90 (5'-C), 55.42 (DMT-OCH_3), 54.01, 48.66, 36.75, 32.19, 32.01, 30.56, 29.96 (20-C), 29.52 (20-C), 28.39 (13-C), 22.96 (23-C), 18.04, 14.39, 12.13 (22-C);

HR-MS (ESI^+): Exact mass calculated for $C_{55}H_{67}N_3NaO_{10}Si$ $[M+Na]^+$: 981.2262, found: 981.0394.

2.4 5'-*O*-(4,4'-Dimethoxytrityl)-2'-*O*-tri-*iso*-propylsilyloxymethyl barbituric acid merocyanine ribonucleoside 3'-(2-cyanoethyl-*N,N*-di-iso-propyl) phosphoramidite S6

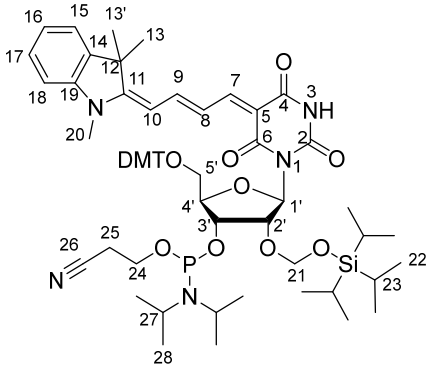

The protected ribonucleoside **S5** (80 mg, 83.9 µmol, 1.00 eq.) was dissolved in dry DCM (1.5 mL) under N_2-atmosphere. DIPEA (141 µL, 668 µmol, 8.00 eq.) and CEP-Cl (33.0 mg, 125 µmol, 1.50 eq.) were added to the mixture which was then stirred at r. t. for 3 h. The solvent was removed in vacuum. Purification of the crude product by column chromatography on silica gel (DCM/MeOH 95:5) yielded the target compound **S6** as a dark purple foam (31 mg, 26.8 µmol, 32%).

^{1}H NMR (400 MHz, $CDCl_3$) δ (ppm) = 8.15 – 8.02 (m, 1 H, 7-H), 7.95 – 7.72 (m, 2 H, 8-H, 9-H), 7.48 (dtd, *J* = 7.9, 3.2, 2.8, 1.3 Hz, 2 H, indole-H), 7.41 – 7.33 (m, 4 H, DMT-H), 7.33 – 7.28 (m, 2 H), 7.26 – 7.20 (m, 2 H), 7.19 – 7.11 (m, 2 H), 6.96 (dd, *J* = 8.0, 3.8 Hz, 1 H), 6.78 (ddt, *J* = 9.0, 7.9, 1.5 Hz, 4 H, DMT-H), 6.44 (s, 1 H, H-1'), 6.02 – 5.89 (m, 1 H, 10-H), 5.08 – 5.01 (m, 1 H), 5.01 – 4.85 (m, 2 H, H-2'), 4.22 – 4.08 (m, 1 H, H-3'), 3.99 – 3.79 (m, 1 H, 24-H), 3.78 – 3.72 (m, 6 H, DMT-OCH_3), 3.53 (dddd, *J* = 15.9, 8.9, 6.9, 3.5 Hz, 2 H, H-5', 24-H), 3.40 (d, *J* = 7.2 Hz, 3 H, 20-H), 3.26 (dtd, *J* = 15.9, 10.0, 6.2 Hz, 1 H, H-4'), 2.75 – 2.61 (m, 1 H, 25-H), 2.36 (dd, *J* = 15.3, 7.8 Hz, 1 H, 25-H), 1.65 (s, 6 H, 13-H), 1.25 (s, 2 H, *i*Pr-CH), 1.13 (td, *J* = 7.9, 7.4, 2.3 Hz, 9 H, *i*Pr-CH_3), 1.06 – 0.95 (m, 23 H, *i*Pr-CH_3);

^{13}C{^{1}H} NMR (100 MHz, $CDCl_3$) δ (ppm) = 171.36 (2-C, 4-C, 6-C), 170.98 (2-C, 4-C, 6-C), 163.32, 162.38, 162.15, 158.36, 156.85 (7-C, 8-C), 156.62 (7-C, 8-C), 145.21, 143.08, 140.35, 136.50, 136.44, 130.39, 130.36 (DMT-C), 128.64, 128.58, 128.53, 127.75, 126.63, 124.06, 122.15 (9-C), 122.05 (9-C), 121.64, 117.96, 117.68, 113.05 (DMT-C), 109.28, 101.07 (10-C), 100.83 (10-C), 89.44, 86.15 (1'-C), 86.10 (1'-C), 81.86 (3'-C), 81.51 (3'-C), 76.41 (2'-C), 75.97 (2'-C), 64.40 (5'-C), 64.25 (5'-C), 59.11 (24-C), 58.92 (24-C), 55.29 (DMT-OCH_3), 55.28 (DMT-OCH_3), 55.26 (DMT-OCH_3), 48.45, 43.42, 43.29, 43.23, 43.09, 31.07, 30.38 (20-C), 29.82, 28.24 (13-C), 24.77 (27-C), 24.70 (27-C), 20.38 (25-C), 20.33 (25-C), 20.27 (25-C), 20.04 (25-C), 19.96 (25-C), 17.93 (23-C), 17.90 (23-C), 12.11 (23-C), 12.09 (23-C), 12.07 (23-C);

^{31}P NMR (162 MHz, $CDCl_3$) δ (ppm) = 149.57, 149.37, 149.23;

HR-MS (ESI$^+$): Exact mass calculated for $C_{64}H_{84}N_5NaO_{11}PSi$ $[M+Na]^+$: 1180.55664 , found: 1180.55492.

3. Synthesis and purification of oligonucleotides

Automated solid phase synthesis was carried using an Applied Biosystems ABI 392 DNA/RNA synthesizer on a 0.6 µmol scale. The following solutions were used: 0.25 M ethylthiotetrazole (ETT) in dry acetonitrile as activator, 3% dichloroacetic acid in 1,2-dichloroethane for detritylation, 20 mM iodine in THF/water/pyridine 66/12/22 for oxidation, pyridine/acetic anhydride/THF 10/10/80 as Cap A solution and 16% NMI in THF as Cap B solution. Syntheses were carried out in DMT-off mode on commercially available CPG solid supports using 70 mM phosphoramidite solutions and a coupling time of 4 min.

Oligonucleotides were cleaved from the solid support and deprotected by incubation in 1.5 mL of water/methanol/triethylamine 5/4/1 for 3 days at ambient temperature. Afterwards, the solid support was filtered off and the solvent was removed in vacuum. The crude samples were redissolved in 1 M TBAF solution in THF (500 µL) and shaken overnight at r. t. After addition of 1 M Tris-HCl pH 8.0 (500 µL), the THF was removed in vacuum and the oligonucleotide samples were desalted by size exclusion chromatography using an Äkta start purification system with three HiTRAP Desalting columns (each 5 mL volume) from GE Healthcare. The desalted oligonucleotides were eluted with water and a flow rate of 2 mL/min. The water was removed under reduced pressure and the samples were redissolved in 600 µL of nanopure water.

PAGE purification of the crude oligonucleotides was performed on 300x200x0.7 mm denaturing polyacrylamide gels (20% acrylamide/bisacrylamide 19:1, 7 M urea) with 1 M TBE buffer (89 mM Tris, 89 mM boric acid, 2 mM EDTA, pH8.3). Gels were run at 35 W constant power for 2.5 h. The oligonucleotides were visualized by UV shadowing on a TLC plate. After excision from the gel, the gel pieces were soaked in TEN buffer (10 mM Tris-HCl, 0.1 mM EDTA, 300 mM NaCl, pH8.0) for oligonucleotide extraction. The pure oligonucleotides were precipitated with absolute ethanol (70% final concentration).

Crude as well as pure oligonucleotides were analyzed by anion exchange HPLC. A Dionex DNAPac PA200 column (2x250 mm) with buffer A (25 mM Tris-HCl, 6 M urea, pH8.0) and buffer B (25 mM Tris, 0.5 M $NaClO_4$, 6 M urea, pH8.0) was used for this quality control. Samples were run with a gradient of 0-48% B over 12 column volumes with a flow rate of 0.5 mL/min and UV detection at 260 nm at an oven temperature of 60 °C. Pure oligonucleotides were additionally analyzed by HR-ESI mass spectrometry, and the monoisotopic masses were obtained by deconvolution of the raw spectra.

4. Spectroscopic characterization

4.1 UV–vis spectroscopy

UV–vis spectra were recorded on an Agilent Cary UV–vis Multicell Peltier spectrophotometer. 5 µM samples were prepared in 1x phosphate buffer (100 mM NaCl, 10 mM phosphate, pH7.0) and measured in semi-micro quartz cuvettes with a path length of 10 mm. Temperature-dependent spectra were recorded in a temperature range of 10 to 90 °C in steps of 10 °C from 200 to 700 nm.

4.2 CD spectroscopy

CD spectra were recorded for 5 µM samples in 1x phosphate buffer (100 mM NaCl, 10 mM phosphate, pH7.0) on a JASCO P-1020 polarimeter with a sodium light source (λ = 589 nm) in a range between 200 and 600 nm. For the measurements, 10 mm semi-micro quartz cuvettes were used.

4.3 Fluorescence spectroscopy

Fluorescence spectra were recorded on a Jasco FP-8300 spectrofluorometer equipped with a FCT-817S cell changer and a Julabo F12 temperature control device. 1 µM samples were prepared in 1x phosphate buffer (100 mM NaCl, 10 mM phosphate, pH7.0) and measured in Hellma ultra-micro quartz cuvettes (10x2 mm). Spectra were recorded with an excitation wavelength of 510 nm (measured emission range 530 to 700 nm) and an emission wavelength of 650 nm (measured excitation range 200 to 630 nm). Excitation and emission bandwidth were both set to 5 nm. Spectra were recorded with 0.1 s response, a PMT voltage of 400 V with 0.5 nm data interval and a scan speed of 1000 nm/min.

The fluorescence lifetimes were determined of highly diluted samples (OD ≤ 0.05) by Time Correlated Single Photon Counting (TCSPC) using a EPL510 pulsed diode laser (λ_{ex} = 506 nm) with a pulse width of 141.7 ps on an FLS980-D2D2-ST spectrometer (Edinburgh Instruments Ltd., UK) under magic angle conditions (54.7°). The photon arrival time was set to 4096 channels and data was collected until 10,000 counts had accumulated in the peak channel. The instrument response function was recorded from colloidal silica as a scatterer by setting the emission monochromator to the peak wavelength of the excitation source. Data fitting was carried out using the Recursive-Fit-routine of the FAST software supplied by Edinburgh Instruments Ltd., Inc. which corrects against the instrument response function (IRF).

4.4 Transient absorption spectroscopy

The output beam of a regenerative Ti:sapphire amplifier system with 1 kHz repetition rate (Solstice, Spectra-Physics, 800 nm, 120 fs) was split using a 50:50 beam splitter to create a pump and a probe arm. One of the beams was used to generate pump pulses with 60 fs duration using a commercial noncolinear optical parametric amplifier (TOPAS White, Light Conversion). For the experiments on rBAM2-D2 and rBAM2^{free}, the central wavelength of the pump pulse was 545 nm and 565 nm, respectively. To obtain pure third-order and fifth-order transient absorption spectra of the dimer, the measurement was conducted at 15 nJ, 45 nJ, and 60 nJ pump pulse energy with the help of a neutral-density filter wheel. The data collected at 15nJ, 45nJ and 60 nJ were averaged over five maps each for better signal-to-noise ratio. For the monomer, the third-order transient absorption map was measured with negligible fifth-order signal contamination by setting a pump-power limit of 15 nJ.

We also used a chopping scheme where we captured the background and the pump-only signals along with the usual pump–probe and probe-only data on a shot-to-shot basis to avoid scattering effects that can contaminate the transient absorption spectra. This was achieved by using a 250 Hz chopper along the probe pulse arm and a 500 Hz chopper along the pump pulse path.

In all measurements, the probe pulse was delayed with respect to the pump pulse using a motorized delay stage (M-IMS600, Newport). The broadband white-light probe pulse was generated by focusing the probe beam into a calcium fluoride (CaF_2) crystal. The probe beam was then focused on the sample position using a focusing mirror (f = 100 mm). The pump and probe beams were spatially overlapped inside a flow cuvette (0.5 mm path length) in which the sample with 0.12 OD absorbance was pumped using a home-built syringe pump apparatus. The pump beam was then blocked behind the sample while the probe beam was spectrally dispersed by a spectrograph (SP2500i, Acton) and then detected using a CCD camera (Pixis 2K, Princeton Instruments).

The procedure for extracting the pure third-order signal, $\mathrm{PP}^{(3)}$, along with the separation of the fifth-order signal, $\mathrm{PP}^{(5)}$, was carried out via

$$\mathrm{PP}^{(3)}I_0 = \mathrm{PP}^{(1Q)}I_0 - 4\,\mathrm{PP}^{(2Q)}I_0, \tag{1}$$

$$\mathrm{PP}^{(5)}I_0^2 = \mathrm{PP}^{(2Q)}I_0, \tag{2}$$

where $PP^{(1Q)}$ and $PP^{(2Q)}$ are single- and double-quantum signals, respectively, that were obtained from the raw pump–probe data, $\mathrm{PP}(I)$. No seventh-order signal was observed. $PP^{(1Q)}$ and $PP^{(2Q)}$ were obtained by using a linear combination of transient absorption data captured at three different intensities, $I = I_0, 3I_0$ and $4I_0$, corresponding to pump-pulse powers of 15 nJ, 45 nJ and 60 nJ, respectively:

$$\mathrm{PP}^{(1Q)} = \tfrac{1}{6}[\mathrm{PP}(4I_0) + \mathrm{PP}(3I_0) - \mathrm{PP}(I_0)] \tag{3}$$

$$\mathrm{PP}^{(2Q)} = \tfrac{1}{6}[\mathrm{PP}(4I_0) - \mathrm{PP}(3I_0) - \mathrm{PP}(I_0)] \tag{4}$$

5. Supporting tables

Table S1 Sequences of RNA oligonucleotides and HR-ESI mass spec data. **X** indicates incorporation of rBAM2.

Number	5'-sequence-3'	Chemical formula	m/z calculated (g/mol)	m/z found (g/mol)
S1	GAUGA**X**AGCUAG	$C_{131}H_{157}N_{50}O_{82}P_{11}$	4082.67716	4082.68706
S2	CUAGCU**X**UCAUC	$C_{126}H_{155}N_{38}O_{86}P_{11}$	3916.60428	3916.62477
S3	CUAGCUAUCAUC	$C_{112}H_{141}N_{40}O_{83}P_{11}$	3714.51558	3714.52176
S4	GAUGAUAGCUAG	$C_{116}H_{142}N_{49}O_{81}P_{11}$	3857.56124	3857.57503

Table S2 Fitting results of lifetime measurements. The lifetime of rBAM2^{free} is below 100 ps and too low to be reliably determined. The two lifetime components observed for the samples could be due to the plausible *cis–trans* isomerization in monomeric ring-open merocyanines.[4,5]

	A_1	τ_1 [ns]	A_2	τ_2 [ns]	$<\tau>$ [ns]
rBAM2^{free}					<0.10
rBAM2-S1	0.52	0.61	0.48	1.69	1.13
rBAM2-D1	0.29	1.40	0.71	2.66	2.29
rBAM2-D2	0.53	0.99	0.47	2.60	1.75

6. Supporting figures

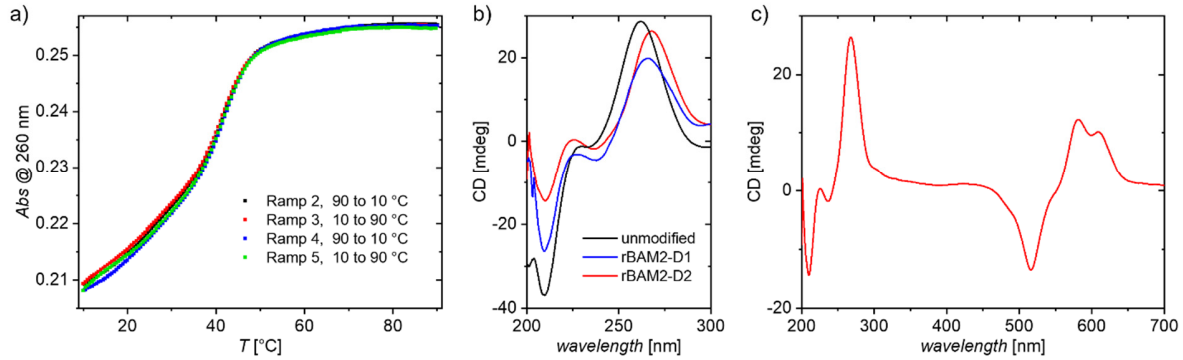

Fig. S1 (a) Melting curves for rBAM2-D2 with two heating and two cooling ramps between 10 and 90 °C. All four ramps of the melting curve are fully overlapping, confirming the integrity of the modified duplex. Any decomposition would result in distorted melting curves. (b) CD spectra in the UV range for unmodified RNA (black), rBAM2-D1 (blue) and rBAM2-D2 (red). (c) Full CD spectrum for rBAM2-D2. Conditions: 5 µM sample in 1x phosphate buffer (100 mM NaCl, 10 mM phosphate, pH7.0), 1 cm pathlength.

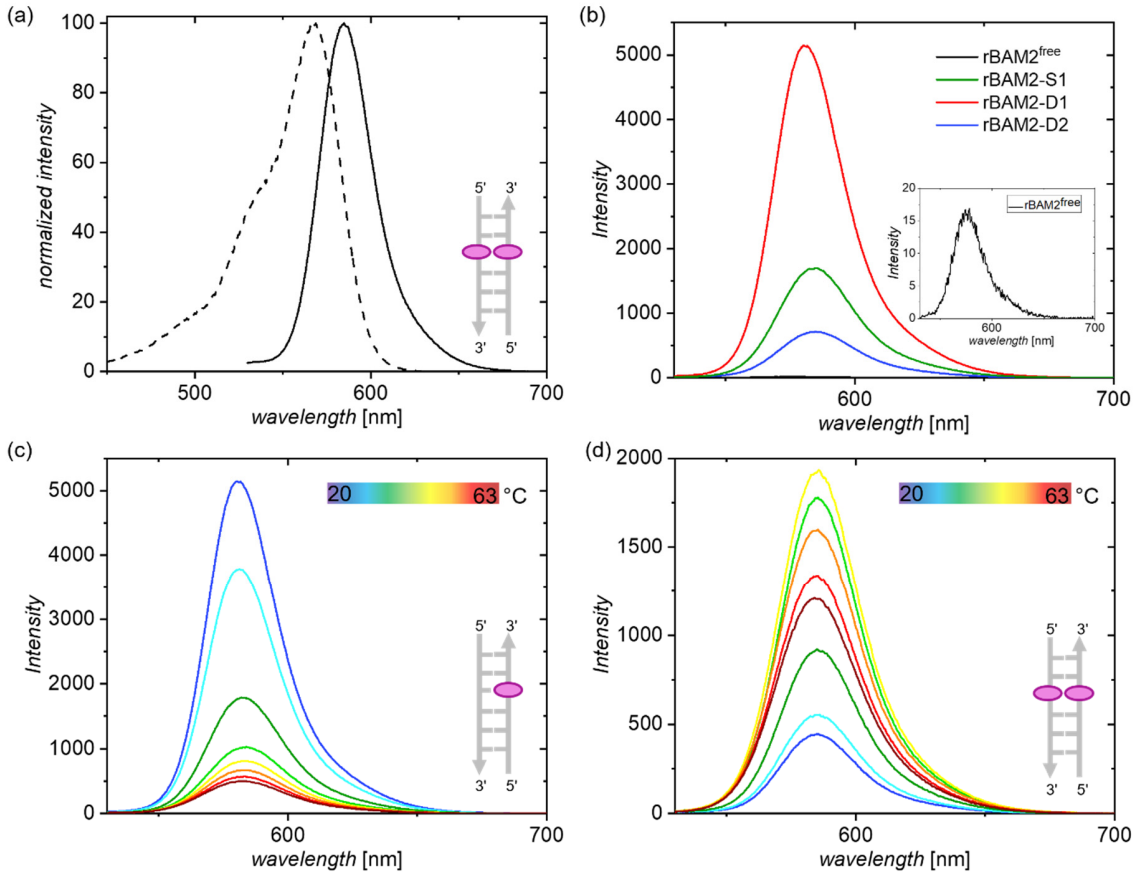

Fig. S2 (a) Normalized steady-state excitation and emission spectra for rBAM2-D2 at 25 °C. (b) Steady-state emission spectra for rBAM2^{free} (black), rBAM2-S1 (green), rBAM2-D1 (red) and rBAM2-D2 (blue). (c) Temperature-dependent emission spectra of rBAM2-D1 for temperatures between 20 °C (blue) and 63 °C (red). (d) Temperature-dependent emission spectra of rBAM2-D2 between 20 °C (blue) and 63 °C (red). Conditions: 1 µM sample in 1x phosphate buffer (100 mM NaCl, 10 mM phosphate, pH7.0), excitation at 510 nm, emission at 650 nm.

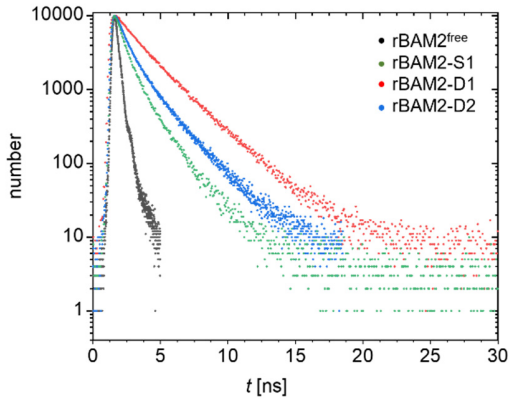

Fig. S3 Fluorescence lifetime data for rBAM2^{free} (black), rBAM2-S1 (green), rBAM2-D1 (red) and rBAM2-D2 (blue) measured by TCSPC at 25 °C. Conditions: sample 1x phosphate buffer (100 mM NaCl, 10 mM phosphate, pH7.0), 1 cm pathlength, 506 nm laser, detection at 585 nm, absorbance of sample <0.05. Amplitude average lifetimes see Table S2.

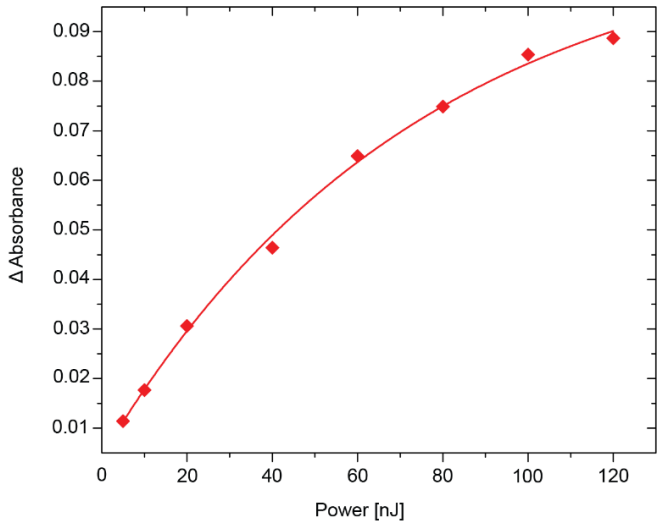

Fig. S4 Pump-power dependence of the maximum change in optical density of the transient absorption spectrum slice at pump–probe overlap (T = 0) for rBAM2-D2 (symbols: data; curve: quadratic polynomial fit).

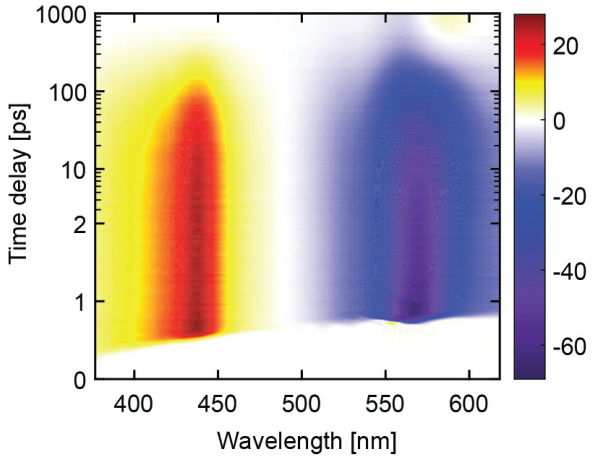

Fig. S5 Third-order transient absorption map of rBAM2^{free}. The negative signal at 565 nm corresponds to ground-state bleach, the positive signal around 440 nm to excited-state absorption and the positive signal at 580 nm emerging at later times to an isomerization photoproduct. The positive transient arises as a result of *cis-trans* isomerization along the free rotating methine bonds of merocyanine.[4, 5] This transient is not observed in rBAM2-D2 dimer due to rigidification of stacking chromophores that hinders isomerization.[6]

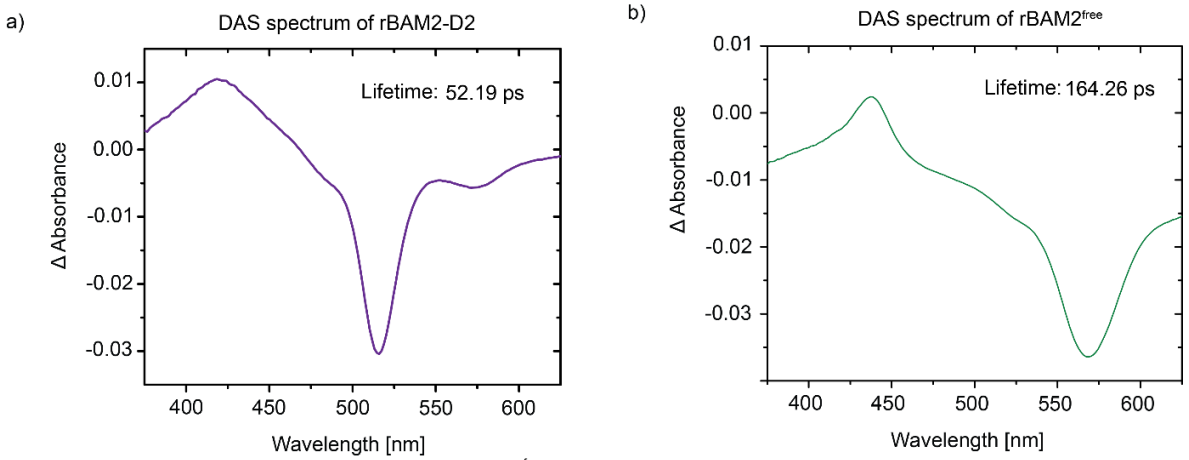

Fig. S6 Decay-associated spectrum (DAS) of (a) rBAM2-D2 and (b) rBAM2^{free}, denoting their respective lifetimes obtained using global analysis in the Glotaran software (version 1.5.1).[7]

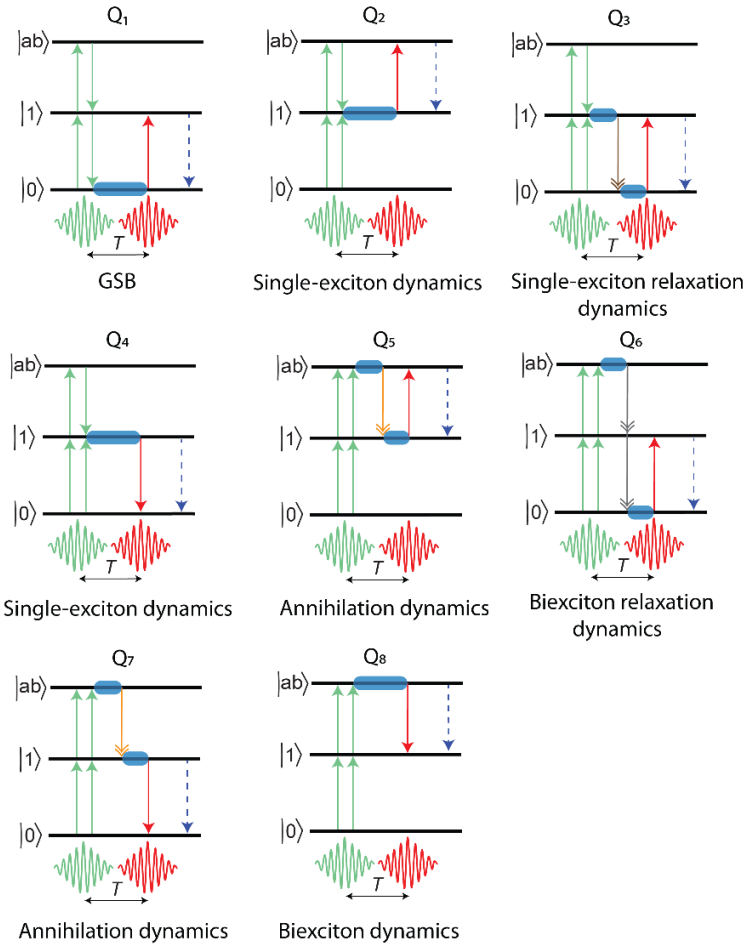

Fig. S7 Energy-ladder diagrams of signal pathways (Q_1 to Q_8) associated with the fifth-order transient absorption signal. There are also other pathways where the time order of interactions is changed and these pathways also include those that originate from two-level systems (not shown).[5] The green arrows indicate the field interactions of the pump pulse (green) creating a population (blue highlight) which is then probed by a broadband pulse (red) at a delay '*T*' indicated by the red arrow. The signal that is detected is indicated by a dashed blue arrow. While Q_1 is a ground-state-bleach (GSB)-like signal pathway that probes a population of the ground state $|0\rangle$, Q_2 and Q_4 represent pathways that probe the dynamics of the single-exciton state $|1\rangle$. Q_3 represents pathway where the probe interacts with the system after it relaxes from $|1\rangle$ to the ground state, indicated by the brown arrow. Q_5 and Q_7 are the annihilation pathways denoting the possibility of probing the system after it relaxes from $|ab\rangle$ to $|1\rangle$. Annihilation is indicated by an orange arrow. Q_6 shows a pathway where the system is probed after the system relaxes from $|ab\rangle$ to $|0\rangle$ denoted by the grey arrow. Q_8 represents a pathway that probes the dynamics of the biexciton state ($|ab\rangle$).

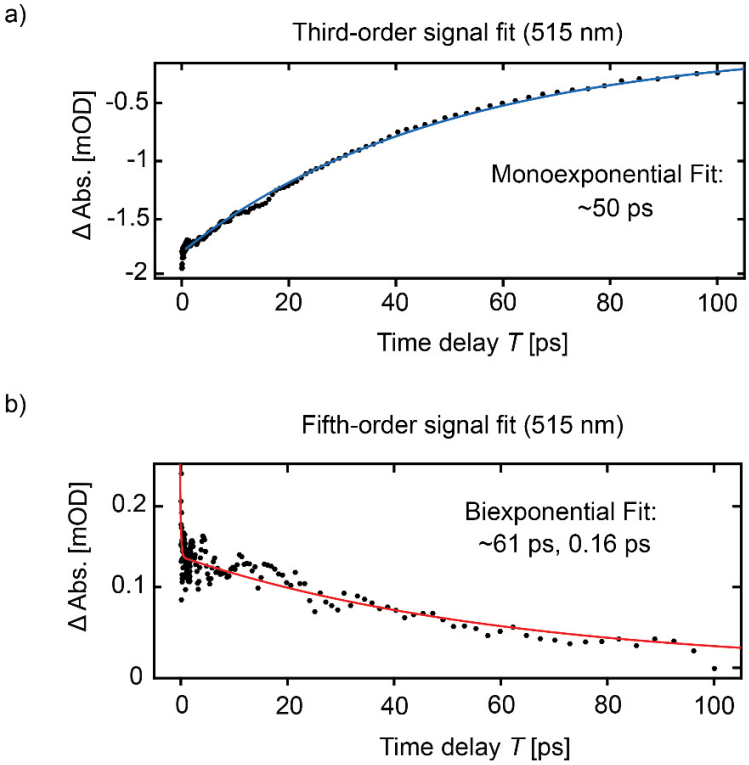

Fig. S8 Kinetic evaluation for rBAM2-D2 taken at a probe wavelength of 515 nm (corresponding to the highest transient signal) for (a) the third-order contribution and (b) the fifth-order contribution. The monoexponential fit (blue colored line) of the data (symbols) in 'a)' reveals the single-exciton lifetime while the biexponential fit (red colored line) of the data (symbols) in 'b)' shows a fast component (0.16 ps) that corresponds to transfer kinetics in the single-exciton manifold in addition to ultrafast exciton–exciton annihilation, while the slow component (61 ps) can be attributed to the single-exciton lifetime. Concerning the fifth-order signal, we did not integrate over the probe axis but rather took a transient slice at the maximum signal of the rBAM-D2 specific signal. This was done to avoid contributions of the rBAM2 monomer that would be introduced upon integration over the probe axis.

7. Supporting data

7.1 HPLC traces of purified oligonucleotides

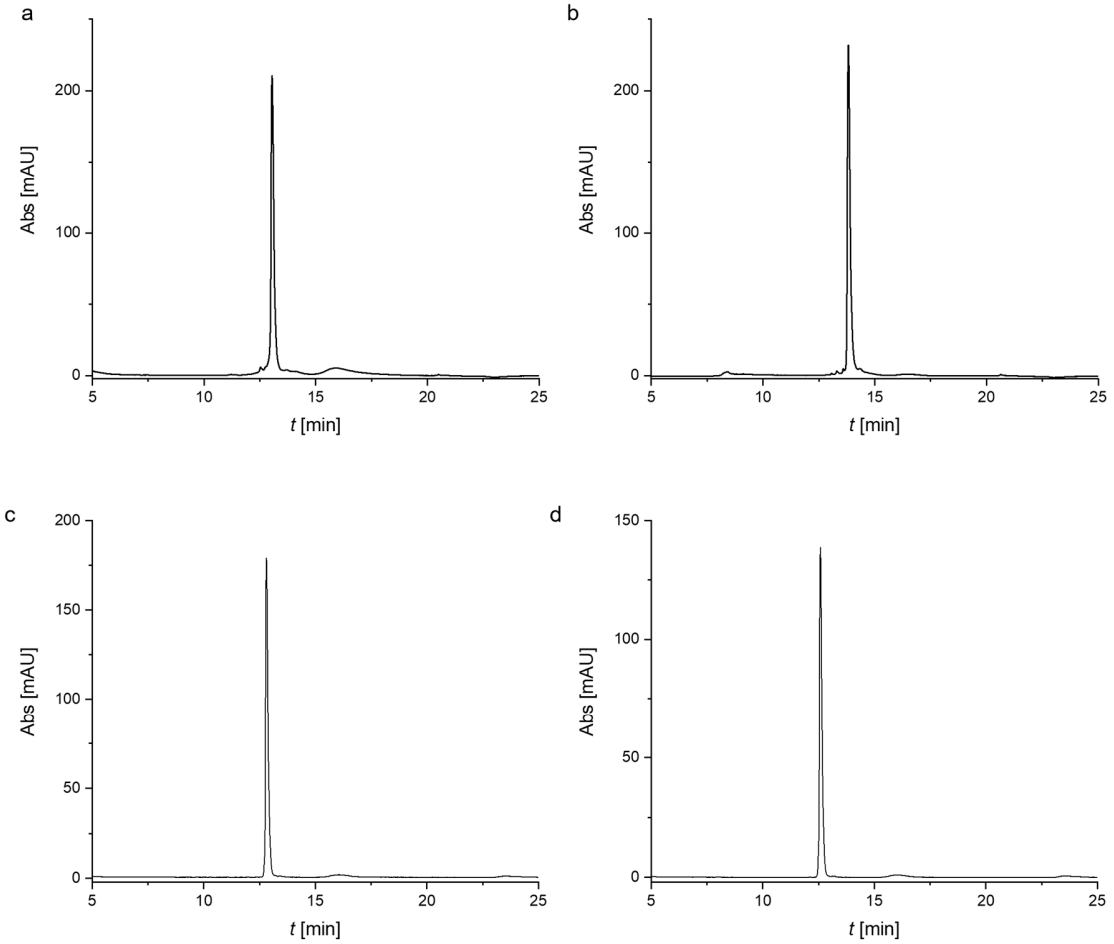

Fig. S9. HPLC traces for pure RNA oligonucleotides: a) S1, b) S2, c) S3, d) S4. Anion exchange HPLC, Dionex, DNAPac PA200, 2x250mm, 60 °C.

7.2 NMR spectra

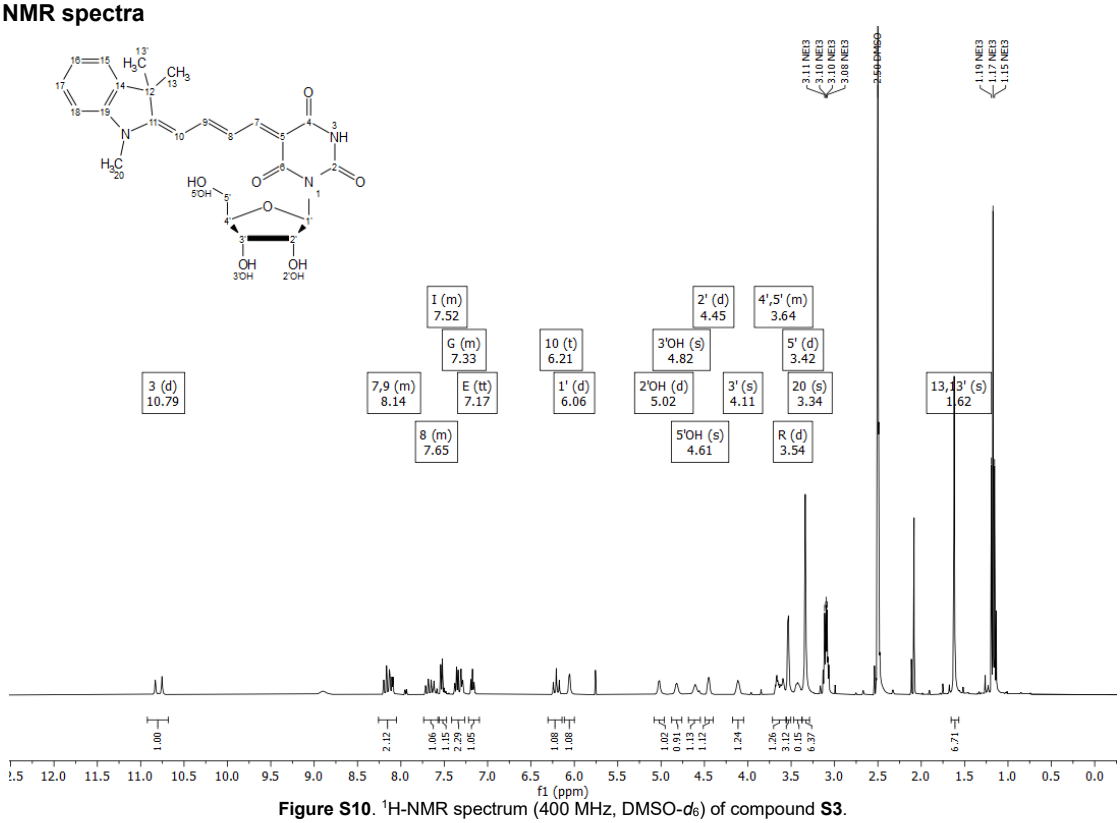

Figure S10. ^{1}H-NMR spectrum (400 MHz, DMSO-d_6) of compound **S3**.

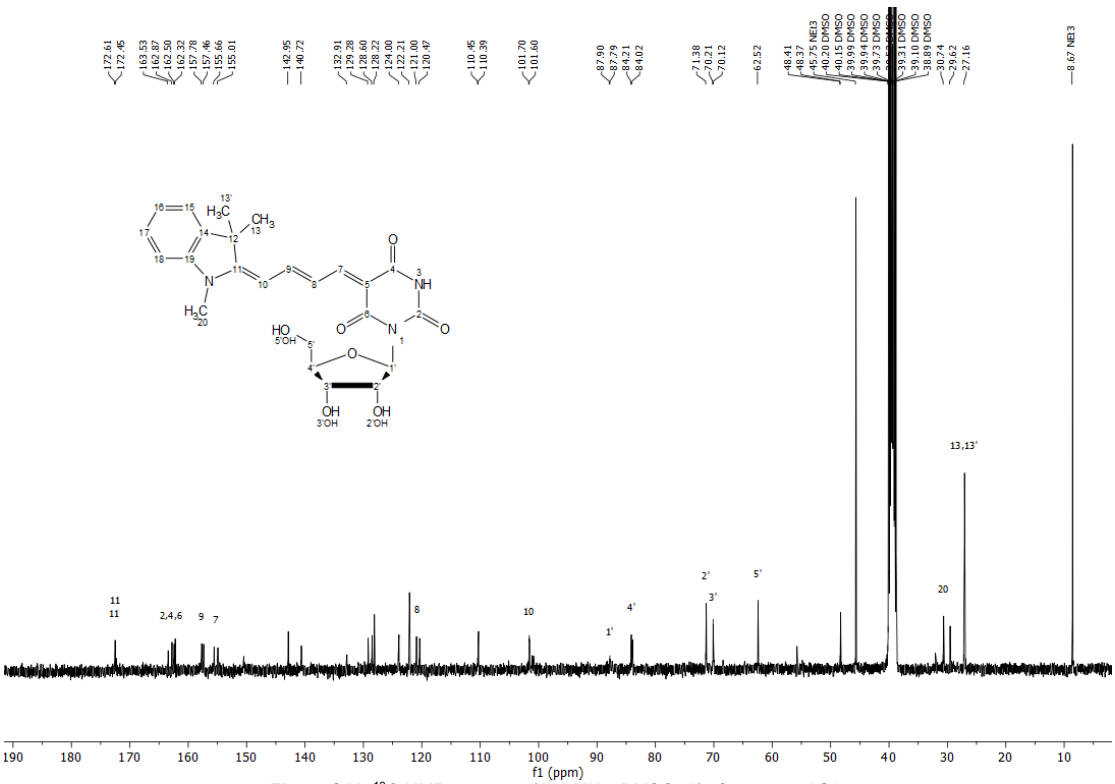

Figure S11. ^{13}C-NMR spectrum (100 MHz, DMSO-d_6) of compound **S3**.

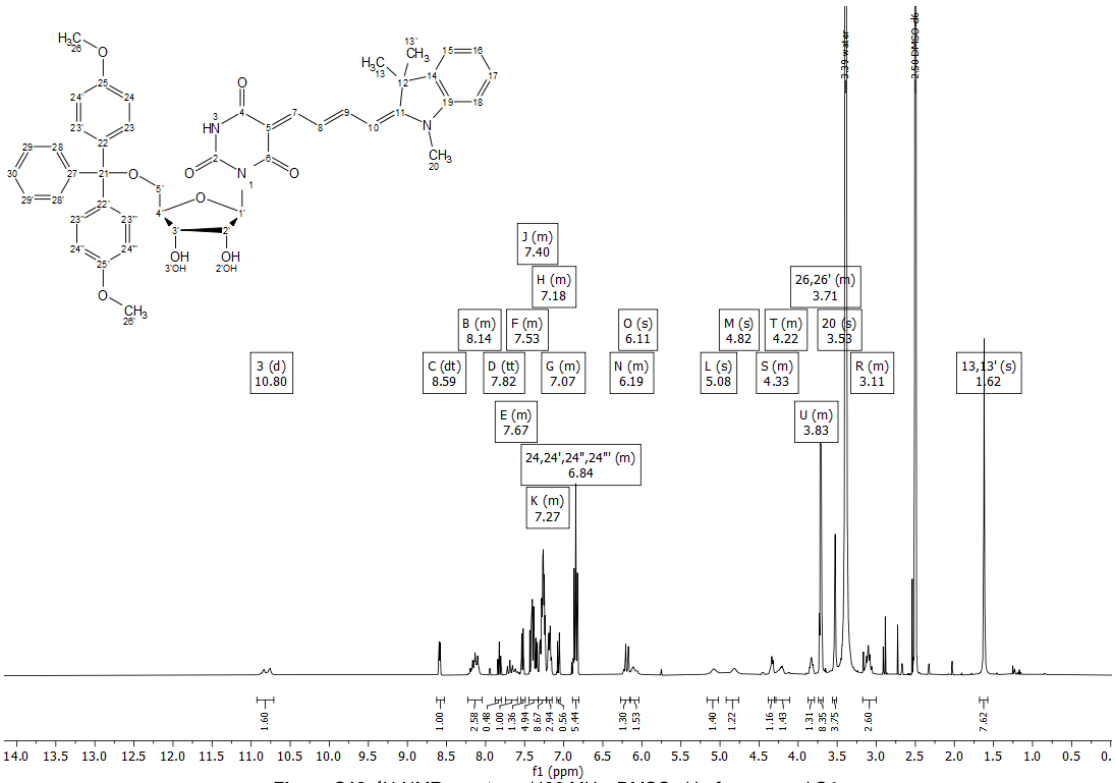

Figure S12. ^{1}H-NMR spectrum (400 MHz, DMSO-d_6) of compound **S4**.

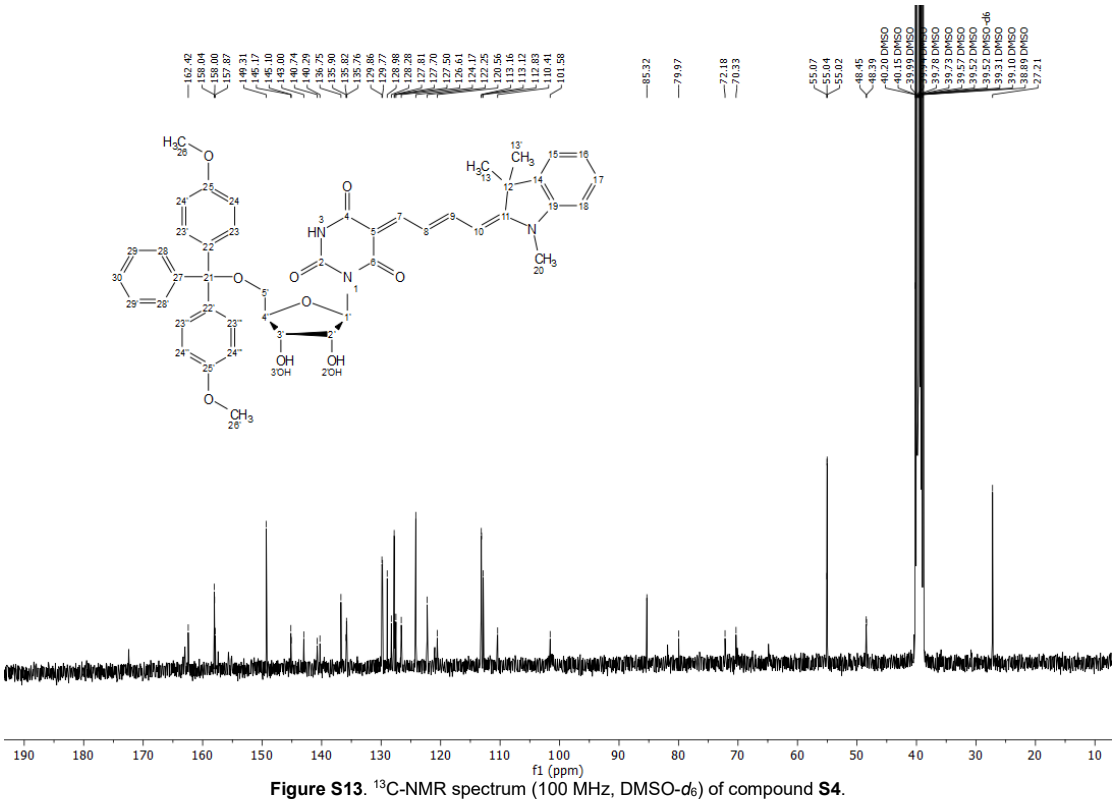

Figure S13. ^{13}C-NMR spectrum (100 MHz, DMSO-d_6) of compound **S4**.

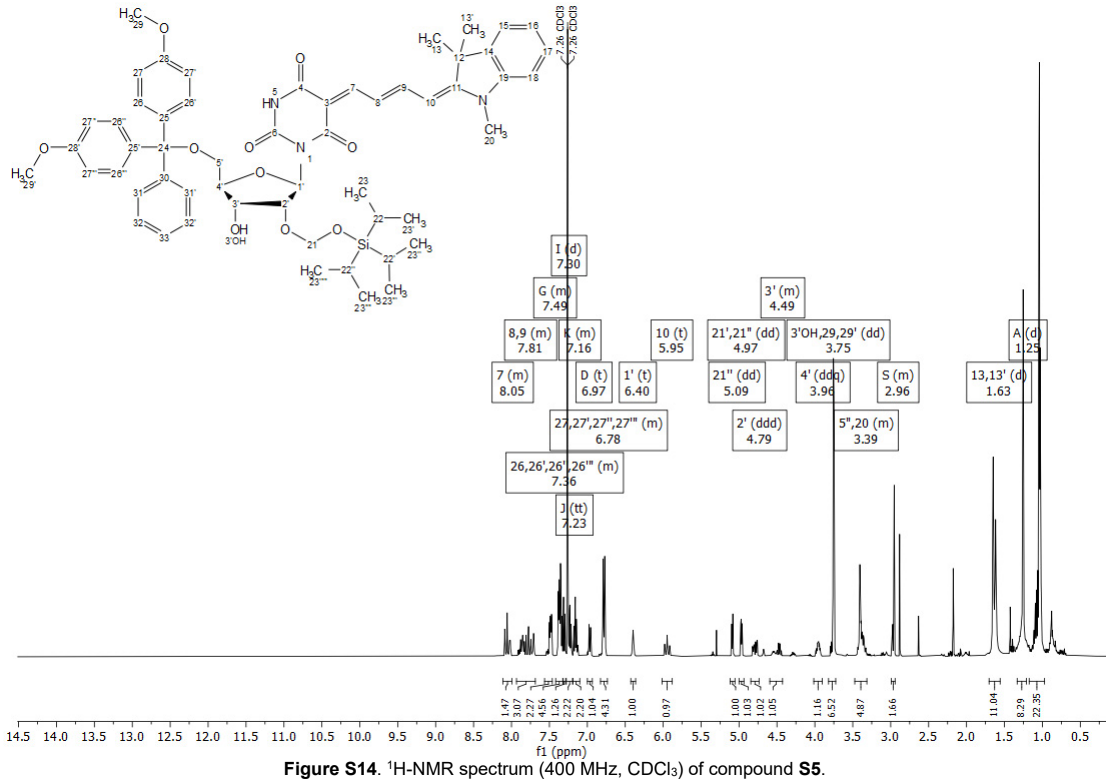

Figure S14. ^{1}H-NMR spectrum (400 MHz, $CDCl_3$) of compound **S5**.

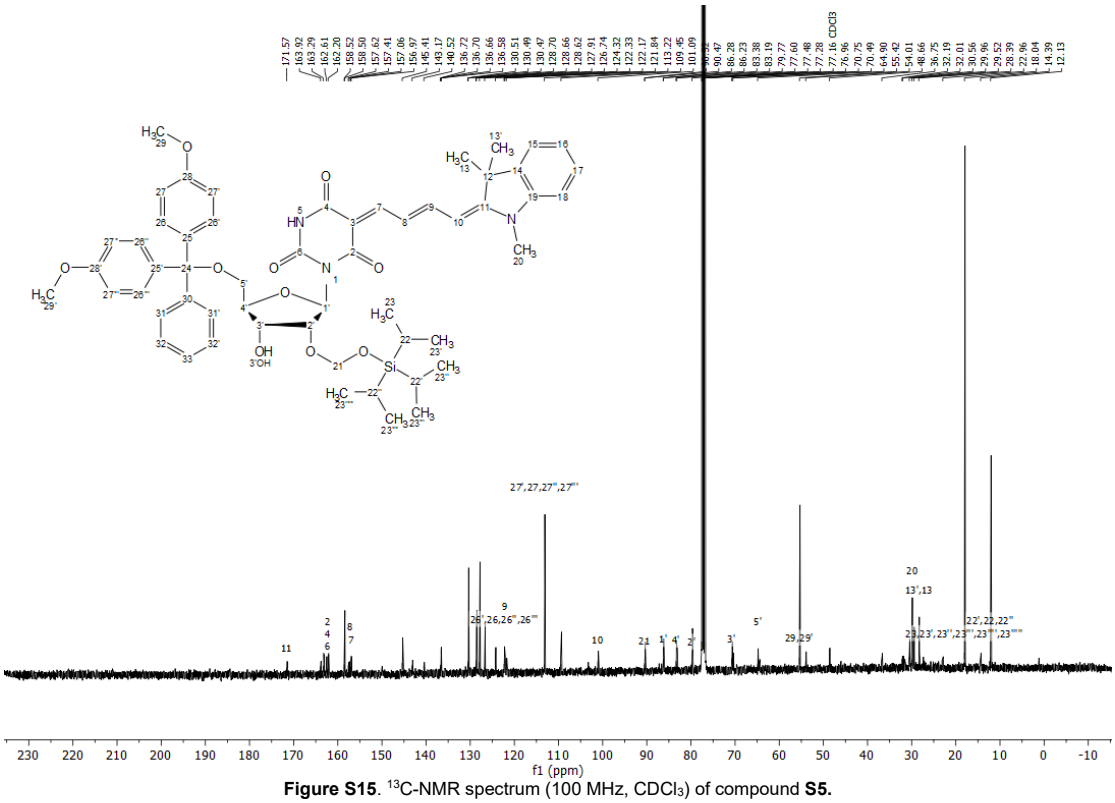

Figure S15. ^{13}C-NMR spectrum (100 MHz, $CDCl_3$) of compound **S5.**

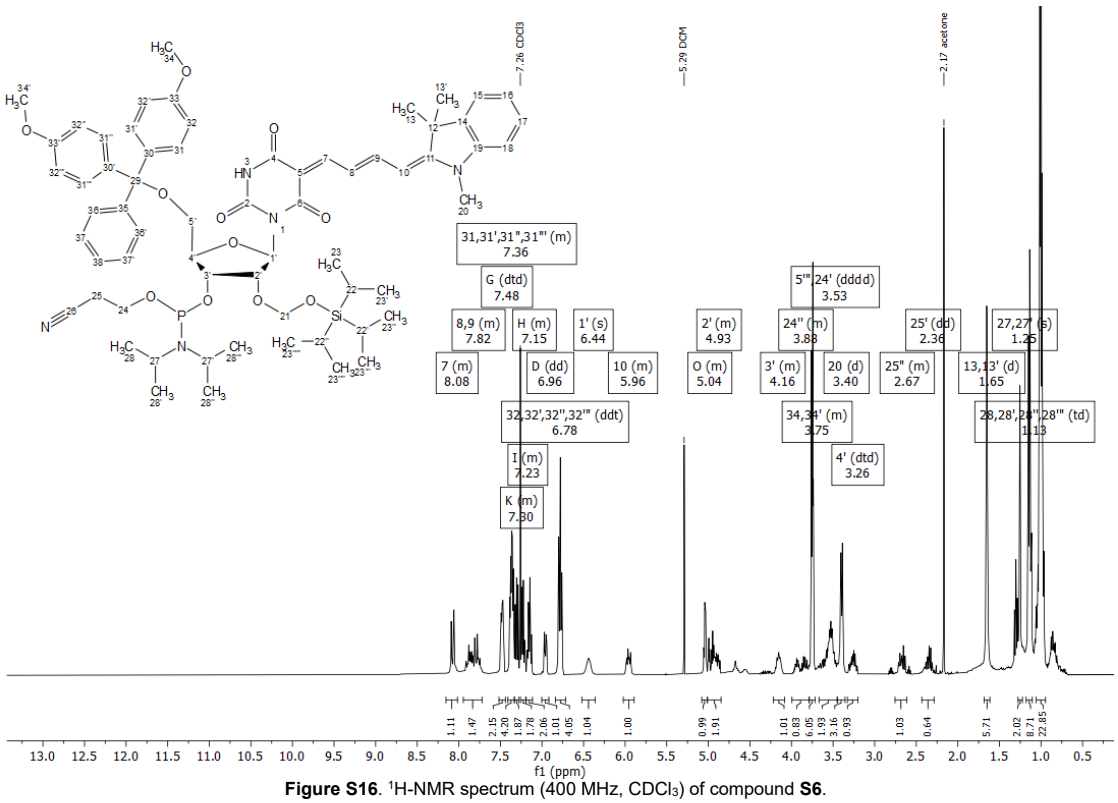

Figure S16. ^{1}H-NMR spectrum (400 MHz, $CDCl_3$) of compound **S6**.

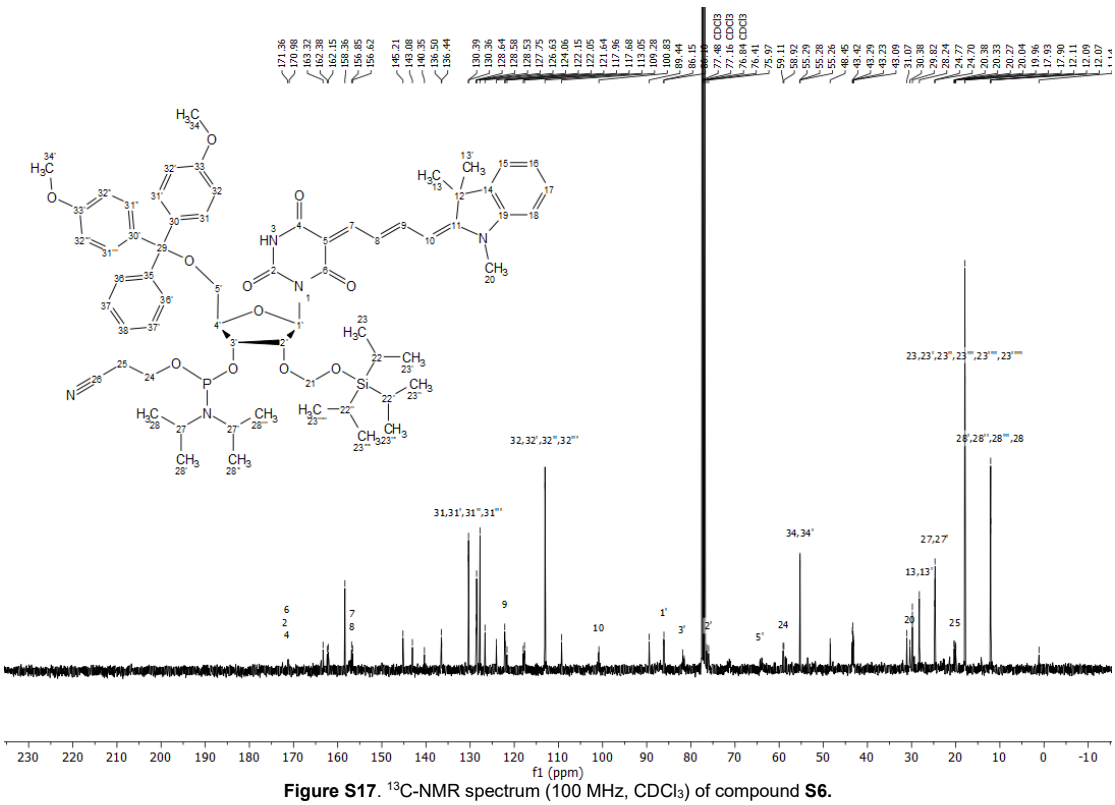

Figure S17. ^{13}C-NMR spectrum (100 MHz, $CDCl_3$) of compound **S6.**

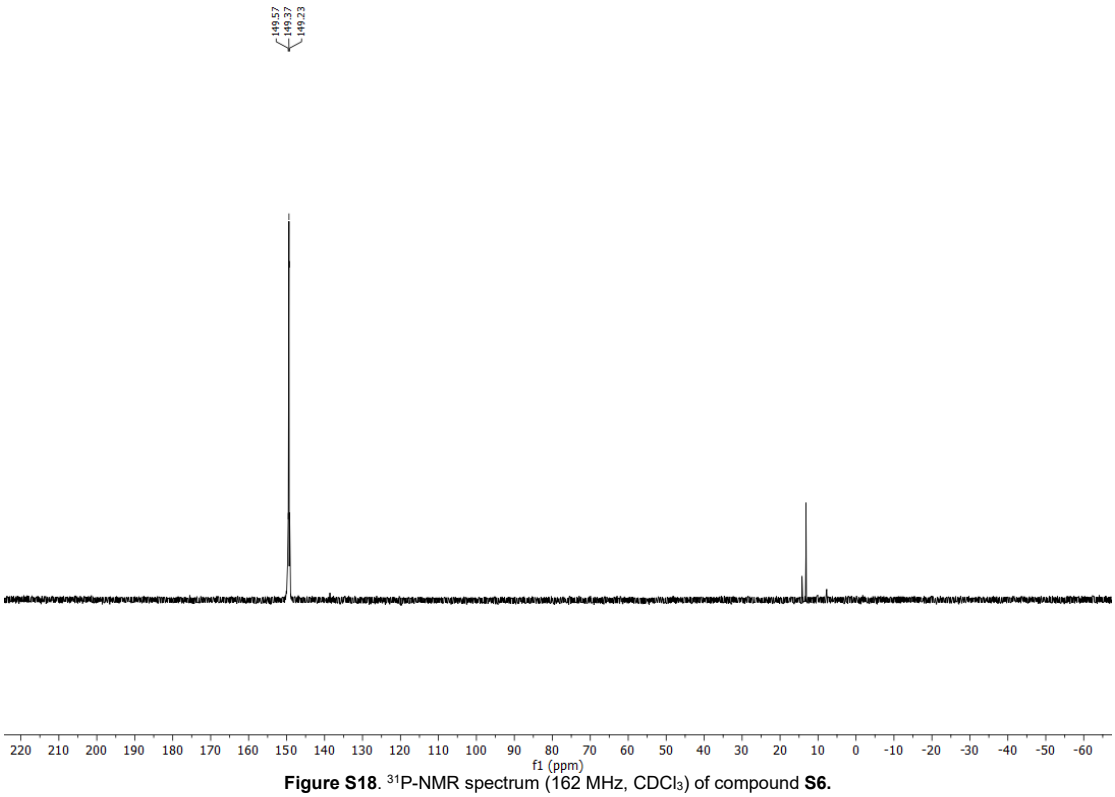

Figure S18. ^{31}P-NMR spectrum (162 MHz, $CDCl_3$) of compound **S6.**

8. References

1. T. E. Kodger, P. J. Lu, G. R. Wiseman and D. A. Weitz, *Langmuir*, 2017, **33**, 6382-6389.
2. R. L. Simmons, R. T. Yu and A. G. Myers, *J. Am. Chem. Soc.*, 2011, **133**, 15870-15873.
3. J. Dietzsch, D. Bialas, J. Bandorf, F. Würthner and C. Höbartner, *Angew. Chem. Int. Ed.*, 2022, **61**, e202116783.
4. C. Walter, S. Ruetzel, M. Diekmann, P. Nuernberger, T. Brixner and B. Engels, *J. Chem. Phys.*, 2014, **140**, 224310.
5. C. Walter, S. Ruetzel, M. Diekmann, P. Nuernberger, T. Brixner and B. Engels, *J. Chem. Phys.*, 2014, **140**, 224311.
6. T. Kim, S. Kang, E. Kirchner, D. Bialas, W. Kim, F. Würthner and K. Dongo, *Chem*, 2021, **7**, 715-725.
7. J. J. Snellenburg, S. P. Laptenok, R. Seger, K. M. Mullen and I. H. M. van Stokkum, *J. Stat. Soft.*, 2012, **49**, 1-22.